Molecular Cell
Article

Structure and Dynamics of the ATP-Bound Open Conformation of Hsp70 Chaperones

Roman Kityk,[1,3] Jürgen Kopp,[2,3] Irmgard Sinning,[2] and Matthias P. Mayer[1,*]
[1]Zentrum für Molekulare Biologie der Universität Heidelberg (ZMBH), DKFZ-ZMBH Alliance, 69120 Heidelberg, Germany
[2]Biochemie Zentrum der Universität Heidelberg, 69120 Heidelberg, Germany
[3]These authors contributed equally to this work
*Correspondence: m.mayer@zmbh.uni-heidelberg.de
http://dx.doi.org/10.1016/j.molcel.2012.09.023

SUMMARY

Central to the chaperone function of Hsp70s is the transition between open and closed conformations of their polypeptide substrate binding domain (SBD), which is regulated through an allosteric mechanism via ATP binding and hydrolysis in their nucleotide binding domain (NBD). Although the structure of the closed conformation of Hsp70s is well studied, the open conformation has remained elusive. Here, we report on the 2.4 Å crystal structure of the ATP-bound open conformation of the *Escherichia coli* Hsp70 homolog DnaK. In the open DnaK structure, the β sheet and α-helical lid subdomains of the SBD are detached from one another and docked to different faces of the NBD. The contacts between the β sheet subdomain and the NBD reveal the mechanism of allosteric regulation. In addition, we demonstrate that docking of the β sheet and α-helical lid subdomains to the NBD is a sequential process influenced by peptide and protein substrates.

INTRODUCTION

The 70 kDa heat shock proteins (Hsp70) form a family of highly conserved molecular chaperones that are present in all domains of life and in most subcellular compartments of eukaryotic cells. Hsp70s, acting in concert with J domain cochaperones and nucleotide exchange factors, assist a multitude of different cellular protein-folding processes during protein maturation and quality surveillance (Kampinga and Craig, 2010; Hartl et al., 2011).

Hsp70 proteins are built up of an N-terminal nucleotide binding domain (NBD) and a C-terminal polypeptide substrate binding domain (SBD). The NBD consists of four α-β subdomains (IA, IB, IIA, and IIB) divided into two lobes by a central ATP binding cleft (Flaherty et al., 1990). The SBD is subdivided into a β sheet subdomain (SBDβ), which contains the peptide binding pocket, and an α-helical subdomain (SBDα), which functions as a lid (Zhu et al., 1996). NBD and SBD are connected via a flexible, highly conserved linker (Bertelsen et al., 2009).

All of Hsp70s' functions rely on the transient interaction of their SBD with a short segment within the substrate polypeptide (Mayer and Bukau, 2005). The affinity of Hsp70s for polypeptides is regulated by the NBD. In the nucleotide-free and ADP-bound state, Hsp70's affinity for substrates is high, but substrate binding and release rates are low. ATP binding increases peptide association and dissociation rates by two and three orders of magnitude, respectively, decreasing the affinity for substrates by 10- to 50-fold (Schmid et al., 1994; Mayer et al., 2000b). ATP hydrolysis is essential for Hsp70 chaperones, but the intrinsic ATPase rate is very low. This ATPase activity is stimulated by protein substrates in synergism with J domain cochaperones (Karzai and McMacken, 1996; Laufen et al., 1999). Thus, NBD and SBD are linked in a mutual allosteric control mechanism, the understanding of which has remained sketchy due to the lack of a structure in which SBD and NBD are properly docked.

Recently, the structure of the yeast Hsp110, Sse1, a distant relative of Hsp70s, was solved and was suggested to represent the open conformation of Hsp70s (Liu and Hendrickson, 2007). However, Hsp110 proteins act as nucleotide exchange factors for Hsp70s (Dragovic et al., 2006; Raviol et al., 2006) and do not seem to require allosteric regulation between domains. Although Hsp110s are able to hydrolyze ATP, at least some of them do not depend on it (Raviol et al., 2006). Therefore, the open conformation of ATP-bound Hsp70s has remained a matter of debate. Here, we solve the structure of the ATP-bound open conformation of the *Escherichia coli* Hsp70 DnaK.

RESULTS

Stabilization of the ATP-Bound Open Conformation of DnaK

Many attempts to determine the structure of the ATP-bound open conformation of Hsp70s have failed in the past, most likely due to their highly dynamic nature. Therefore, we strived to stabilize the open conformation by using a disulfide bond. On the basis of a homology model of DnaK using the Sse1 structure as a template and on hydrogen-exchange data (Figure S1 available online), we created double-cysteine variants of DnaK by introducing cysteines at position 47 in the NBD and at different positions along helix B of the SBD, between positions 525 and 541. In addition, we removed the last 32 residues, which are known to be highly flexible and are not essential for the in vivo and in vitro function of DnaK (Zhu et al., 1996), and replaced them with a hexahistidine tag. We tested the constructs in vivo for complementation of the temperature sensitivity phenotype

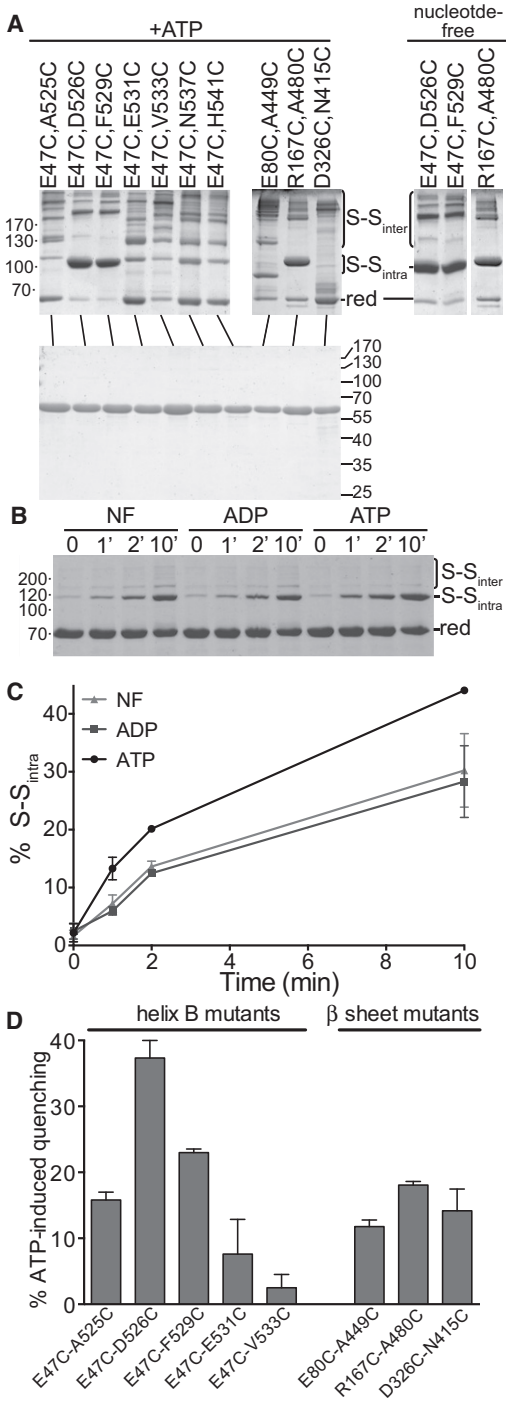

Figure 1. Intramolecular Disulfide Formation and Fluorescence Quenching Support an Sse1-like Open Conformation

(A) Different double-cysteine DnaK variants were oxidized with Cu(II)-(1,10-Phenanthroline) in the presence of ATP and separated by SDS-PAGE. In the reduced form (red), DnaK runs at 66 kDa, DnaK with intramolecular disulfide (S-S_{intra}) at 100 kDa. Intermolecular crosslinks are denoted as S-S_{inter}. Right panel, disulfides can also be formed in the nucleotide-free state. Lower panel, reduced double-cysteine DnaK variants.

(B and C) Kinetics of disulfide-bond formation of DnaK-E47C,D526C in different nucleotide states.

(B) Representative Coomassie blue-stained SDS-PAGE gel of the oxidation products.

(C) Quantification of the results obtained from the oxidation-kinetics experiment shown in (B). Error bars represent the SEM of three independent experiments.

(D) ATP binding induces a distance-dependent self-quenching of fluorescence of HiLyte Fluor 488-labeled double-cysteine DnaK variants (see Figure S3). The relative quenching, as (fluorescence in the absence of ATP − fluorescence in the presence of ATP) ÷ the fluorescence in the absence of ATP, is blotted. The error bars are SEM of at least three measurements.

of a *ΔdnaK* strain and found that all DnaK constructs were fully functional (data not shown).

We then tested which of these DnaK variants could form an intramolecular disulfide in the presence of ATP (Figure 1A). We took advantage of the fact that DnaK species with intramolecular crosslink appear on SDS gel as bands with a higher molecular weight than that of wild-type DnaK. Intramolecular disulfide bond formation was also verified by using electrospray-ionization mass spectrometry (Figure S2). DnaK-E47C,D526C and DnaK-E47C,F529C formed an intramolecular disulfide in the presence of ATP with much higher efficiency than other variants. This is consistent with the $DnaK^{Sse1}$ model, wherein Asp526 and Phe529 are closest to Glu47 as compared to other residues in helix B (Table S1).

To further validate our model, we searched for positions in NBD and SBDβ suitable for disulfide bonds. The closest distances were found between residue pairs E80-A449, R167-A480, and D326-N415 (Table S1). Only DnaK-R167C,A480C formed a disulfide bond efficiently in the presence of ATP (Figure 1A).Taken together, the disulfide crosslinking results support our model of the open conformation.

DnaK Can Assume an Open Conformation in the Nucleotide-free State

We next asked whether the open, Sse1-like conformation is only accessed in the ATP-bound state or also in the nucleotide-free state. Disulfides between SBDα and NBD (47–526 and 47–529) and between SBDβ and NBD (167–480) also formed efficiently in the absence of nucleotide (Figure 1A, right panel). This is very surprising, because nuclear magnetic resonance data suggested that NBD and SBD are instead disjoined in the absence of ATP (Swain et al., 2007; Bertelsen et al., 2009). Our finding demonstrates that docking of helix B and SBDβ to the NBD also occurs in the nucleotide-free state. This result is consistent with recently published data, which indicate that in all nucleotide states of the Hsp70s, "open" and "closed" conformations coexist, though in different proportions (Marcinowski et al., 2011; Schlecht et al., 2011). We resolved the oxidation kinetics for DnaK-E47C,D526C and found that ATP accelerated intramolecular disulfide formation roughly 2-fold and decreased the fraction of intermolecular crosslinks (Figures 1B and 1C).

ATP Binding Decreases the Average Distance between SBD Subdomains and NBD

This result poses the question of whether the observed open conformation is related to the ATP state or whether it is a rare conformation of all states trapped by disulfide formation. To

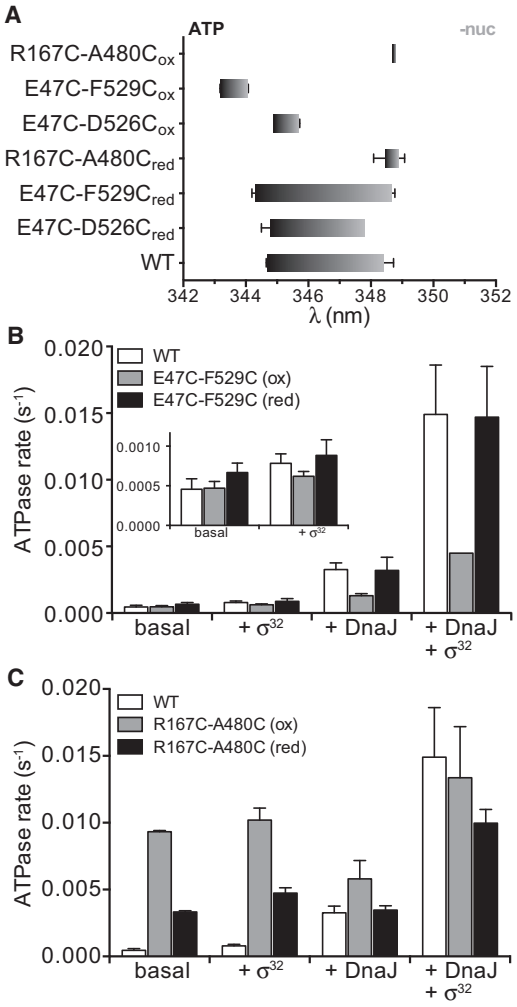

Figure 2. Tryptophane Fluorescence and ATPase Activity of Cross-linked DnaK Variants

(A) Tryptophane fluorescence of oxidized (ox) and reduced (red) DnaK variants. The right and left borders of the bar indicate the fluorescence-emission maximum in the nucleotide-free (-nuc) and ATP-bound (ATP) states, respectively. The size of the bar indicates the size of the ATP-induced blueshift. Error bars are SEM of at least three measurements. WT, wild-type.

(B and C) Single-turnover ATPase activity of DnaK-E47C,F529C (B) and DnaK-R167C,A480C (C) in the absence of any cofactors or in the presence of DnaJ (50 nM), σ^{32} (1 μM), or a combination of both in the reduced and oxidized states, as indicated. Inset in (B) is a zoom of the data for basal and σ^{32}-stimulated ATPase rates. Error bars are SEM of at least three measurements.

address this question, we attempted to determine whether the respective residues are closer in the ATP state than in the ADP state using fluorescence spectroscopy. We had previously found that two molecules of the environment-sensitive dye HiLyte Fluor 488 quench each other's fluorescence when in close proximity (Graf et al., 2009). Using polyprolyl peptides as a molecular ruler, we show now that fluorescence quenching is observed when two dyes are closer together than 16 Å (Figure S3). As shown in Figure 1D, the equilibrium fluorescence intensity of double-labeled DnaK variants is quenched upon the addition of ATP, and the extent of this quenching correlates well with the distances measured in our homology model (Table S1), taking the orientation of the respective residues and the linker between the thiol attachment and the center of the dye into consideration.

Tryptophane Fluorescence

To further validate that the disulfide-bonded DnaK variants represent a conformation prevalent in the ATP-bound state, we used tryptophane fluorescence. DnaK has a single tryptophane situated in the NBD (Trp102; see Figure S1), which responds to ATP-induced conformational changes with a shift of the maximum of fluorescence emission by 3–4 nm toward shorter wavelengths (Theyssen et al., 1996). This shift is not observed when helices A and B are deleted (Moro et al., 2003), suggesting that helix B comes into close proximity with Trp102.

Reduced DnaK-E47C,D526C and DnaK-E47C,F529C had wild-type-like tryptophane spectra, with an emission maximum in the nucleotide-free state of around 348 nm (right end of the bar shown in Figure 2A) and an ATP-induced blueshift of ~4 nm (size of the bar in Figure 2A). Interestingly, the maximum in tryptophane fluorescence of oxidized DnaK-E47C,D526C and DnaK-E47C,F529C was already strongly shifted toward a shorter wavelength in the absence of ATP, and the emission maximum was in a region comparable to wild-type DnaK in the presence of ATP, indicating that linking helix B to the NBD leads to changes in Trp102's surroundings similar to those induced by binding of ATP. Addition of ATP to the oxidized form of DnaK-E47C,D526C and DnaK-E47C,F529C shifted the emission maximum by about 1 nm further, to a shorter wavelength.

In contrast to helix B double-cysteine constructs, DnaK-R167C,A480C did not exhibit a significant ATP-induced blueshift in either the reduced or the oxidized state. The maximum of fluorescence was positioned around 349 nm, which corresponds to the emission maximum of wild-type DnaK in the nucleotide-free state. This result was not surprising, given that it was shown previously that Arg167 is engaged in interdomain communication and that replacement of this residue leads to a loss of allostery (Vogel et al., 2006). These results indicate that linking of SBDβ to the NBD does not automatically lead to docking of SBDα with the NBD.

ATPase Activity

To verify the functionality of the DnaK constructs, which formed an intramolecular disulfide bond, we determined the ATPase activity under single turnover conditions. Wild-type DnaK had a very low intrinsic ATPase rate of 5×10^{-4} s^{-1}, consistent with published data (McCarty et al., 1995). This rate could be stimulated 1.7-fold by 1 μM of the natural substrate heat-shock transcription factor σ^{32} of *E. coli* and ~7-fold by low concentration of DnaJ (50 nM). In the presence of σ^{32} and DnaJ, a 32-fold synergistic stimulation was observed, consistent with earlier results (Laufen et al., 1999). Both oxidized and reduced forms of DnaK-E47C,F529C hydrolyzed ATP with a basal rate similar to wild-type DnaK (Figure 2B). Reduced DnaK-E47C,F529C responded to the ATPase stimulation both by DnaJ alone and together with the substrate in a wild-type-like manner. The ATPase activity of oxidized DnaK-E47C,F529C was also

Table 1. Diffraction Data and Refinement

Crystal Parameters	
Space group	C2
Cell dimensions	a = 202.33 Å, b = 77.47 Å, c = 182.96 Å, $\alpha = \gamma = 90^\circ$, $\beta = 101.7^\circ$
Cell content	4 protein molecules/AU
Solvent content	52%
Data Collection	
Wavelength	0.9792 Å
Resolution	59.7 Å – 2.40 Å (2.47 Å – 2.40 Å)
Unique reflections	108,315
R_{sym}	8.8% (49%)
Average I/σ	5.2 (1.6)
Completeness	99.7% (100%)
Redundancy	3.2 (3.2)
Refinement	
R_{work}/R_{free}	19.6% / 23.9%
Average B factor	70.6 $Å^2$
Rmsd bond ideality	0.009 Å
Rmsd angle ideality	1.099°
Ramachandran favored	97.5%
Protein residues	2392
ATP:Mg^{2+}	4
Water	514

AU, asymmetric unit; rmsd, root-mean-square deviation. Values in parentheses indicate the corresponding statistics in the highest-resolution shell.

stimulated by the substrate and DnaJ, albeit to a lesser extent (1.4-, 3-, and 10-fold for σ^{32}, DnaJ, and σ^{32}+DnaJ, respectively). Oxidized DnaK-E47C,F529C is clearly competent for hydrolysis of ATP and for response to the signals of DnaJ and substrate.

DnaK-R167C,A480C in the reduced state showed 7-fold-increased basal ATPase activity in comparison with wild-type DnaK (Figure 2C), and stimulation by DnaJ alone was not observed, consistent with data implicating Arg167 in interaction with DnaJ (Suh et al., 1998). Unexpectedly, oxidized DnaK-R167C,A480C had a basal ATPase rate of $9.2 \times 10^{-3}\ s^{-1}$, which is close to the values observed for the wild-type protein when stimulated synergistically by DnaJ and σ^{32}. Obviously, oxidation of this DnaK variant results in a conformation that brings in close proximity residues from SBDβ and NBD that are necessary for full stimulation of the ATPase activity.

Structure of the Open Conformation of DnaK

Because all functional data indicated that linking SBDα to the NBD produces a conformation similar to the one prevalent in the ATP-bound state, we tried to solve the structure of this conformation. To crystallize DnaK in the ATP-bound open conformation, we combined the cysteine replacements E47C,D526C and E47C,F529C with the Thr199 to alanine replacement (T199A) in the nucleotide binding pocket. The T199A replacement reduces the ATPase activity at least 10-fold but retains wild-type-like allosteric regulation between NBD and SBD (Barthel et al., 2001; Rist et al., 2006).

Both oxidized triple-amino-acid replacement variants were used in crystallization trials in the presence of ATP, but only DnaK-E47C,T199A,F529C yielded suitable crystals. The structure was solved by molecular replacement and refined at 2.4 Å resolution to an R value of 19.9% (R_{free} = 23.6%; Table 1). There were four DnaK·ATP molecules in the asymmetric unit, forming two head-to-head symmetric dimers (Figure S4). The four DnaK molecules have fairly distinct crystal-packing contacts but their structures are highly similar, indicating that the observed structure is not compromised by crystal packing.

To test whether DnaK·ATP is also a dimer in solution, we performed size-exclusion chromatography coupled to static light scattering (Figure S4) with oxidized and reduced DnaK-E47C,T199A,F529C in the presence of ATP. Even at high concentrations of 50 μM, only very little dimer was found, which argues against a hypothesis that the dimeric conformation found in the crystals is a physiologically relevant state.

Overall Structure of DnaK·ATP and Comparison to Sse1 and to DnaK·ADP

In the ATP-bound open conformation, DnaK is composed of three folding units, the NBD and the two subdomains of the SBD, SBDβ, and SBDα, which are detached from each other and contact different sides of the NBD (Figure 3A). The NBD shows the typical actin-like fold found in Hsp70s and the structure of all four subdomains (IA, IB, IIA, and IIB) are highly similar to previously solved structures, but their orientation relative to each other is significantly different. The SBDβ forms a two-layered β sandwich with upward protruding loops and contacts the NBD subdomains IA, IB, and IIA. The SBDα consists of four helices, the first of which is bound to the side of NBD subdomain IB as expected from the disulfide bond between position 47 and 529. This overall arrangement of the DnaK·ATP structure resembles the previously solved Sse1 structure (Figure 3B) (Liu and Hendrickson, 2007). However, there are significant differences, which are important for the allosteric coupling of NBD and SBD in Hsp70s. The most striking difference is the orientation of the SBDβ, which is moved upward by about 20° and sideways toward the subdomain IIA by 25° as compared to Sse1 (Figure 3B). As discussed in detail below, there are six polar contact sites in DnaK between SBDβ and NBD, of which only three are found in Sse1. Additional differences are found in the position of the NBD subdomains relative to each other and in the SBD subdomains (Supplemental Information).

Compared to the solution structure of DnaK in the ADP state (Bertelsen et al., 2009), the differences are much more pronounced (Figure 3C). In the ADP state, NBD and SBD appear as two separate units that do not seem to contact each other (Swain et al., 2007), and helices A and B of SBDα are packed tightly onto SBDβ. In the ATP state, helices A and B form a continuous helix. The difference in the NBD between DnaK·ATP and DnaK·ADP is also much more substantial than the differences between DnaK and Sse1 NBDs.

Nucleotide Binding Domain

Many structures of isolated NBDs of Hsp70s in the absence of nucleotides and in the presence of ADP, ATP, or AMP-PNP have been solved in the past twenty years. Surprisingly, all of

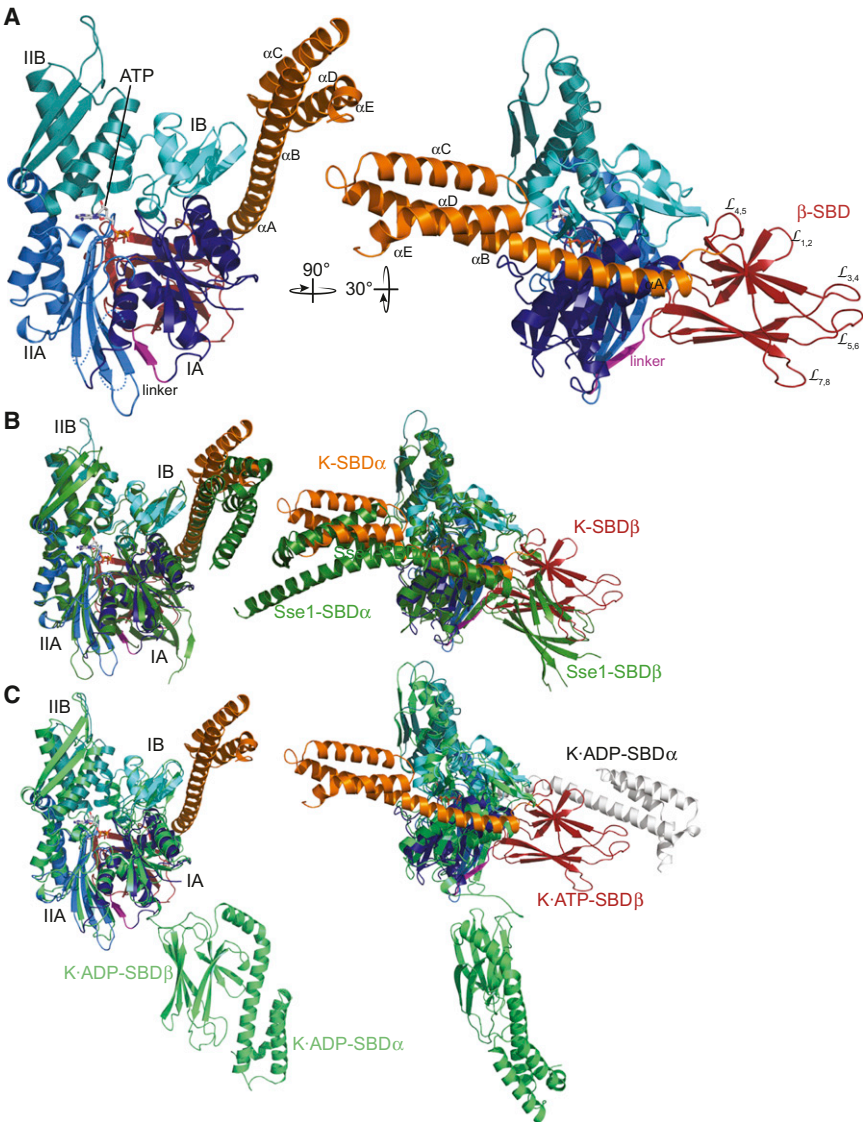

Figure 3. Crystal Structure of ATP-Bound DnaK in the Open Conformation

(A) Ribbon diagram of DnaK·ATP in the front and side views, colored according to the subdomains as follows: NBD subdomain IA, dark blue; IB, cyan; IIA, light blue; IIB, dark teal; NBD-SBD linker, magenta; SBDβ, brown; and SBDα, orange. Bound ATP is shown as sticks. Loops and helices in the SBD are denoted according to Zhu et al. (1996).

(B) Overlay of the DnaK·ATP and Sse1 structures (PDB ID code 2QXL, Liu and Hendrickson, 2007). Coloring of DnaK is as in (A); Sse1 subdomains are colored in dark green.

(C) Overlay of DnaK·ATP and DnaK·ADP (PDB ID code 2KHO, Bertelsen et al., 2009). DnaK·ADP is colored in light green. In the side view, the SBDα of the closed conformation of the SBD (PDB ID code 1DKX, Zhu et al., 1996) is overlaid (light gray) to indicate the orientation of the SBDβ of DnaK·ATP.

these structures were very similar and did not reveal major ATP-induced conformational changes. In contrast, the structure of the NBD in the ATP-bound state is quite different from any of these (Figure S5). To visualize the differences in subdomain orientation in the NBD, we overlaid structurally corresponding Cα atoms of subdomain IIA of DnaK·ATP with DnaK·ADP and projected the superimposed Cα traces into all three planes in space (Figure 4A). In standard view (x-y plane) lobe I is rotated counterclockwise, resulting in closure of the nucleotide binding cleft and widening of the lower crevice (Figure 4A, front). When looking at lobe I from the right side (y-z plane, Figure 4A, side IA-IB), it becomes apparent that lobe I is also rotated in this plane counterclockwise relative to lobe II, reducing the twist between the two lobes. Viewing subdomains IA and IIA from the top (x-z plane) reveals that subdomain IA is again rotated counterclockwise, and this rotation is even more pronounced in subdomain IB (Figure 4A, top IA-IIA and top IB-IIB). All three rotations add together to position subdomain IA closer to SBDβ by 6 to 9 Å and to move parts of subdomain IB by about 12 Å into the cleft above ATP (Figure 4A). This movement opened a cleft between subdomains IA and IIA on the front side of the NBD and changed the interface for SBDβ and SBDα (Figure 4B, Movie S1).

ATP is coordinated by residues from all four subdomains (Figures 4C and 4D). A Mg^{2+} ion in the active center coordinates β- and γ-phosphate in a bidentate complex, suggesting that ATP is in a position poised for γ-phosphate cleavage. Consistent with a very low or absent ATPase activity for the DnaK-T199A variant (Barthel et al., 2001), none of the water molecules are positioned for the inline attack on the γ-phosphate to initiate hydrolysis. Surprisingly, Lys70 is at hydrogen-bond distance to the γ-phosphate, suggesting a different mechanism for γ-phosphate cleavage than proposed previously (see Discussion).

Substrate Binding Domain

The SBDβ of our structure deviates in four important points from the previously solved structure of the isolated SBD of DnaK (Protein Data Bank [PDB] ID code 1DKX; Zhu et al., 1996) (Figures 5A–5C). First, β strand 8 is rotated by 180° and hydrogen bonds with strand 5 of the upper β sheet of the two-layered β sandwich instead of strand 7 of the lower sheet. Therefore, the upper β sheet consists of five strands (2, 1, 4, 5, and 8), and the lower only of three (3, 6, and 7). Second, the upper β sheet is much more twisted; consequently, the substrate binding cleft between strands 1 and 4 is wider by about 10°. Third, the angle between the upper and lower β sheet is decreased by 10° to 20°, apparently increasing the conformational freedom of the outer loops $L_{3,4}$ and $L_{5,6}$, which enclose the substrate peptide in the previous structure and which are not completely resolved in two of the four molecules in our

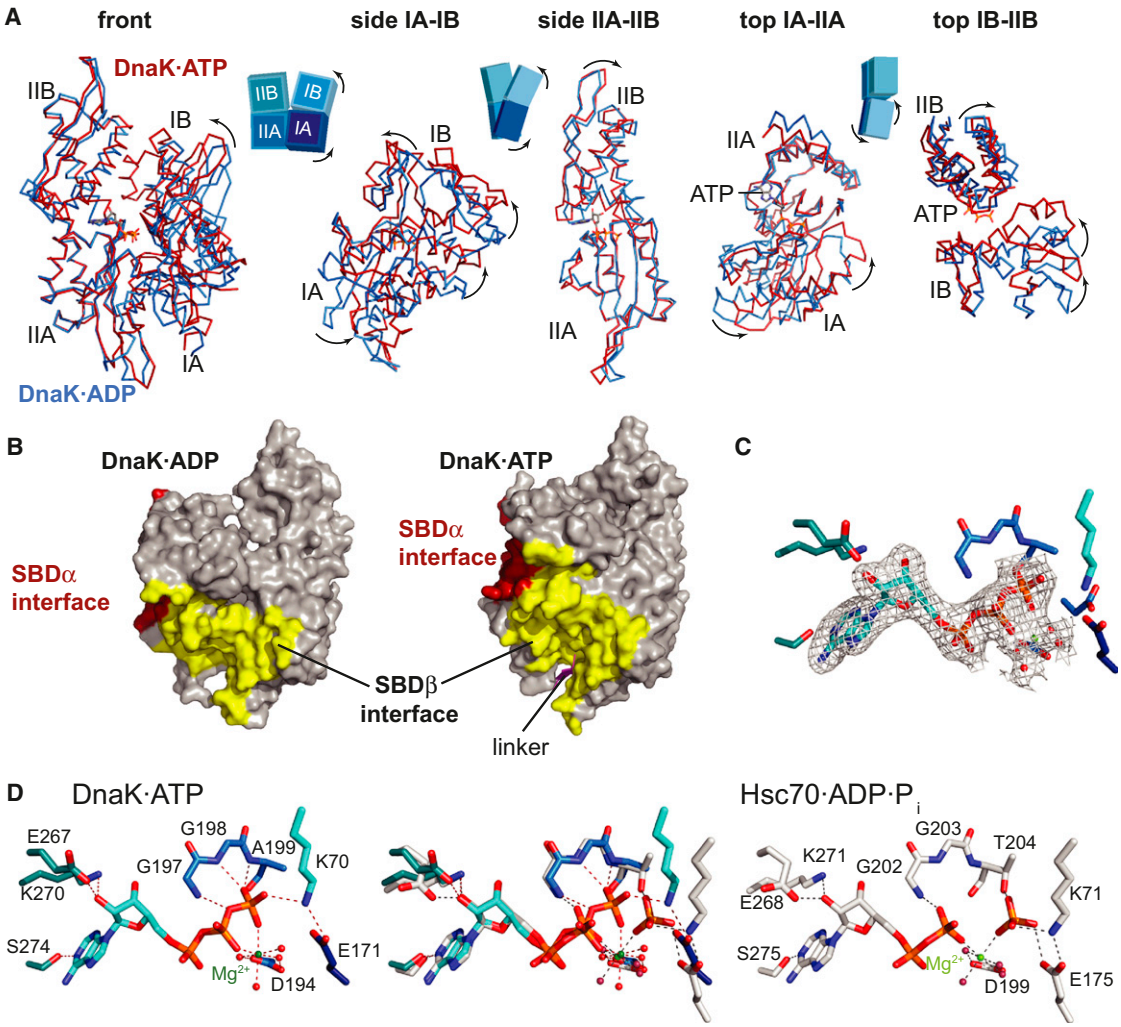

Figure 4. ATP Binding Induces Substantial Displacements in the NBD Subdomains of DnaK

(A) Overlay of NBD Cα traces of DnaK·ATP (red) and DnaK·ADP (blue, PDB ID code 2KHO). ATP-induced subdomain movements are indicated with arrows. Insets indicate orientation of the domain and major displacement directions (see Movie S1).

(B) Surface representation of DnaK·ATP NBD and DnaK·ADP NBD. The interface with linker and SBDβ is colored in yellow and the interface with SBDα is colored in red.

(C) $2F_{obs}$-F_{calc} electron-density map around ATP, Mg^{2+}, and Mg^{2+}-coordinated water molecules at 1.0 σ.

(D) Comparison of pre- and posthydrolysis states in the catalytic center of Hsp70s. Nucleotide and coordinating residues are shown as sticks. Carbonyl and amides of the peptide backbone are only shown if involved in binding. For better clarity, Asp8, Thr11, Thr12, and Asn13 (Asp10, Thr13, Thr14, and Tyr15 in Hsc70), which coordinate the β-phosphate, are omitted. Dashed lines indicate hydrogen-bonding distance. Left panel, coordination of ATP in DnaK·ATP. Residues are colored according to the element and the NBD subdomain they belong to (IA, dark blue; IB, cyan; IIA, light blue; and IIB, dark teal). Right panel, coordination of ADP and phosphate in bovine Hsc70 (PDB ID code 1HPM, Wilbanks and McKay, 1995). Middle panel, overlay of left and right panels.

structure. Fourth, the hydrophobic pocket in the SBDβ, which is tailored for binding a single hydrophobic residue, is much smaller in our structure than in the previous substrate-containing structure (Figure 5C). The minimal distance between the side chains of the pocket-lining residues Phe426 and Ile438 is reduced by almost 3 Å (see Supplemental Information).

Except for the missing kink between helices A and B, the SBDα is very similar to the previous structure of DnaK's isolated SBD (root-mean-square deviation = 0.839 Å, helices B–E). In contrast, it deviates significantly from the SBDα of Sse1 (Figure 3B).

NBD-SBD Contacts

The interaction surface between SBDβ and the NBD involves three of the four subdomains of the NBD (IA, IB, and IIA). Of the SBDβ, six regions are involved in the interactions: the highly conserved linker between NBD and SBD, the loop $L_{2,3}$, the end of β strand 4, the loop $L_{6,7}$, strand 7, and the linker between strand 8 and the SBDα. The interdomain linker hydrogen bonds with strand 13 of the NBD, thereby extending the central β sheet of subdomain IIA. Linker residue Asp393 is in hydrogen-bond (H-bond) distance to Asn170 and Thr173 of the loop between

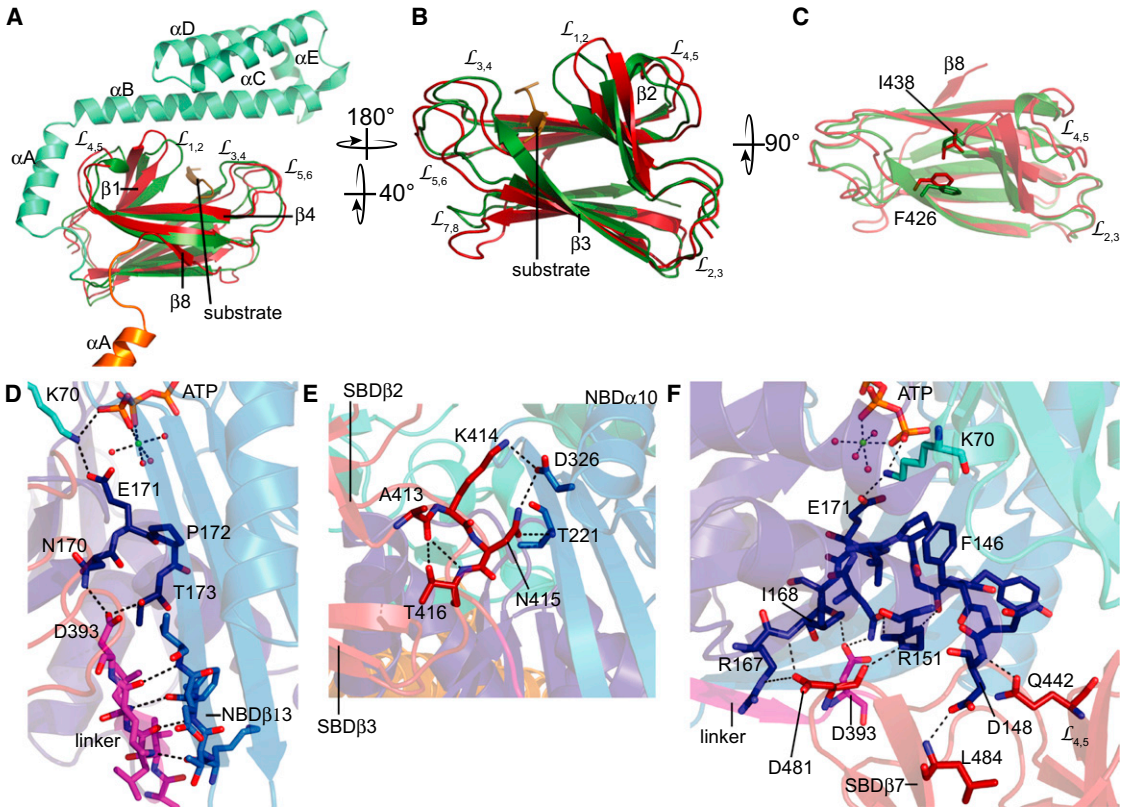

Figure 5. ATP-Induced Rearrangements in the SBD and Interdomain Contact Sites Important for Allostery

(A–C) Substrate-enclosing loops are more distant from the substrate binding pocket in DnaK·ATP than in the substrate-containing structure of isolated SBD. Overlay of the isolated SBD of DnaK (green; PDB ID code 1DKX, Zhu et al., 1996) with the SBDβ of DnaK·ATP (red) in a ribbon diagram. SBDα of DnaK·ATP (orange) is truncated for space reasons.

(B) SBDβ of the same overlay as in (A), but rotated 180°.

(C) SBDβ overlay rotated 90° as compared to (B). Substrate binding pocket lining residues F429 and I438 are shown as sticks (see Movies S2 and S3).

(D–F) Details of interdomain contact sites. Dashed lines indicate H-bond distance.

(D) Interaction of the highly conserved NBD-SBD linker (magenta) with the central β sheet of subdomain IIA (light blue) and Asp393 with Asn170 and Thr173 of subdomain IA (dark blue).

(E) Interaction of Lys414 and Asn415 (SBDβ $L_{2,3}$) with Asp326 and Thr221 (NBD IIA).

(F) Polar contacts between Gln442 (SBDβ $L_{4,5}$) with Asp148 backbone (NBD IA), I484 (SBDβ β strand 7) with Asp148 side chain, and Asp481 (SBDβ $L_{6,7}$) with Arg151, Arg167, and I168 (NBD IA).

strand 10 of the central β sheet of subdomain IA and the last helix of IA, which crosses over to subdomain IIA (Figure 5D). The second site involves Lys414 and Asn415 of loop $L_{2,3}$ of the SBDβ and Asp326 at the end of helix 10 of subdomain IIA (Figure 5E). In addition, Asn415 is at H-bond distance to the backbone amide of Thr221 of strand 13 of the NBD. The third contact is formed between Gln442 from the end of β strand 4 of SBDβ and the backbone amide of Asp148 (IA) (Figure 5F). The fourth interaction involves the side chain of Asp481, which is at H-bond distance to the backbone of Ile168 and forms a polar contact with Arg167 (Figure 5F). In addition, Arg151 hydrogen bonds to the backbone carbonyl of Asp481. The fifth site is formed between the side chain of Asp148 (IA) and the backbone amide of Leu484 in strand 7 of SBDβ (Figure 5F). Finally, Ser505 and Gly506 of the linker between SBDβ and SBDα contact Asn98 and Asp100 in subdomain IB. As discussed in the Supplemental Information, many of the sites involved in interdomain contacts were previously found to be involved in allosteric regulation. Only three of the six NBD-SBD contact sites are found in Sse1 (Supplemental Information), which suggests why Sse1 does not possess an allosteric mechanism similar to Hsp70s.

Dynamics of the Open Structure

Resolving the Kinetics of the ATP-Induced Conformational Changes in DnaK

Because our fluorescent probes were responsive to ATP-induced distance changes between SBDα and NBD IB and SBDβ and NBD (Figure 1D), we decided to resolve the kinetics of these conformational changes in DnaK. As shown above, ATP binding causes three major rearrangements: (1) complete relocation of helix B and its docking to the NBD; (2) docking of the β sheet subdomain of SBD to NBD; and (3) binding of the interdomain linker in a hydrophobic groove of the NBD. Until now, the sequence of these events was not resolved. To solve

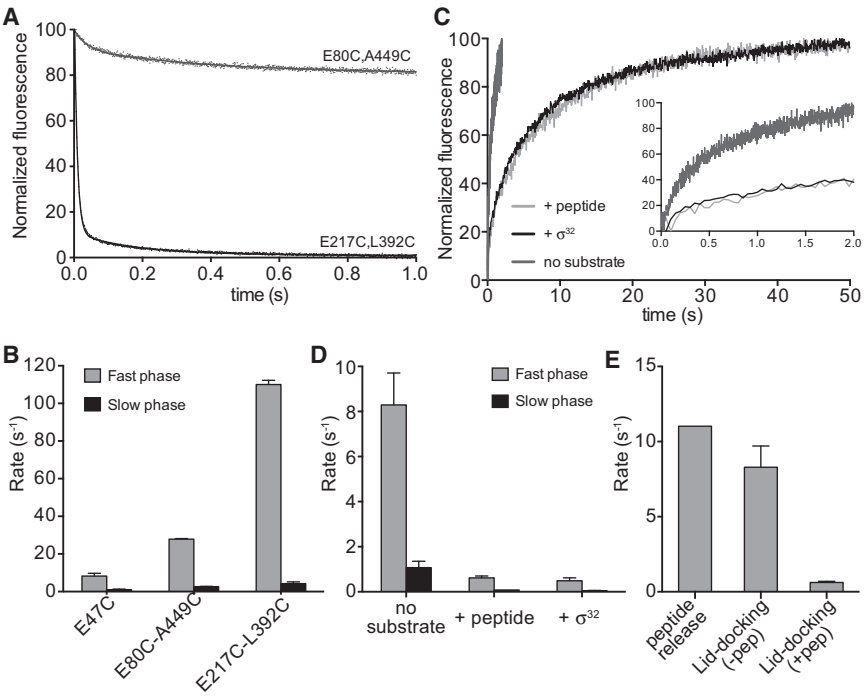

Figure 6. Fluorescence Reveals the Kinetics of ATP-Induced Conformational Changes

(A) Kinetics of the ATP-induced linker-NBD and SBDβ-NBD docking for HiLyte Fluor 488-labeled DnaK-E217C,L392C and DnaK-E80C,A449C. Solid lines are double-exponential fits to the data.

(B) Docking of linker and SBDβ to NBD precedes docking of SBDα and NBD. ATP-induced fluorescence change of HiLyte Fluor 488-labeled DnaK-E47C, DnaK-E217C,L392C, and DnaK-E80C,A449C was determined as in (A), and the data were fit with double-exponential models.

(C and D) Bound-protein and peptide substrates decrease the rate of SBDα-NBD docking. Nucleotide-free HiLyte Fluor 488-labeled DnaK-E47C was preincubated with NR-peptide (NRLLLTG) or σ^{32} for at least 30 min before the complex was rapidly mixed with a large excess of ATP.

(C) Individual fluorescence traces. The inset is a zoom into the first 2 s of the kinetics.

(D) Rates of fast and slow phases of a double-exponential fit to the data.

(E) Comparison of the rates for ATP-induced NR-peptide release and ATP-induced SBDα-NBD docking for DnaK-E47C variant in the absence (-pep) and presence (+pep) of a peptide. Error bars are SEM of at least three measurements.

this problem, we used labeled DnaK variants and followed the change in fluorescence as a function of time using a stopped-flow device. Of the three β sheet double-cysteine variants, only DnaK-E80C,A449C behaved like wild-type DnaK in ATPase activity and ATP-induced substrate release. Therefore, we used this variant to measure the docking kinetics of SBDβ to NBD.

We could not use E47C-D526C and E47C-F529C to determine the docking rates of helix B to the NBD, because Asp526 and Phe529 are important for the proper mechanics of the SBD, and their replacement by cysteine leads to increased substrate release rates (Schlecht et al., 2011; Figure S7). Instead, we used HiLyte Fluor 488-labeled DnaK-E47C, which had wild-type-like substrate release rates (Figures S7B and S7C) and showed an increase in fluorescence upon the addition of ATP due to the dye's sensitivity to polarity changes in its vicinity. In addition, we used DnaK-E217C,L392C to measure docking of the linker into the hydrophobic groove of the NBD.

All three reactions—ATP-induced docking of SBDβ, linker, and helix B to the NBD—followed double-exponential kinetics with a fast phase of 8.3 s^{-1} (SBDα), 27.9 s^{-1} (SBDβ), and 107 s^{-1} (linker) (Figure 6B). These results indicate that, upon ATP binding, first the linker inserts into the hydrophobic groove of the NBD and then the SBDβ binds, followed by helix B. This suggests that relocation of helix B depends on the docking of the linker and SBDβ to the NBD.

Substrates Affect the Mechanics of the Helical Lid

We wondered whether peptide and protein substrates bound to DnaK would have any effect on the ATP-induced relocation of helix B. It was shown previously that the lid is in a more open position when a protein substrate is bound as compared to a bound peptide substrate (Schlecht et al., 2011). We used labeled DnaK-E47C to prepare complexes with NR-peptide (NRLLLTG) and σ^{32}. Then, we rapidly mixed the DnaK-substrate complexes with ATP and followed the increase of fluorescence with time (Figure 6C). Both NR-peptide and σ^{32} strongly decreased the ATP-induced docking of helix B to the NBD (Figure 6D).

We also compared the kinetics of the ATP-induced dissociation of a peptide using a fluorescent-labeled variant of NR-peptide and ATP-induced helix B-to-NBD docking (Figure 6E). To our great surprise, the peptide release rate was 18-fold higher than the rate for docking of the lid to the NBD in the presence of a peptide. Thus, at the moment when helix B docks onto NBD, the substrate is already released from DnaK.

DISCUSSION

In this study we solved several key issues of the molecular mechanism of Hsp70 chaperones. We found that in ATP as well as in ADP and the nucleotide-free state, Hsp70s can assume an open conformation with SBDα detached from SBDβ, and both subdomains of the SBD dock onto different sides of the NBD. The inter-NBD-SBDβ contacts revealed by our structure suggest an allosteric mechanism of interdomain communication—in particular, how substrate binding can influence ATP hydrolysis. In addition, our structure indicates a catalytic mechanism for γ-phosphate cleavage that is different from the previously proposed mechanism. Our kinetic measurements demonstrate that the highly conserved interdomain linker first inserts into a hydrophobic groove between subdomains IA and IIA of the NBD, then SBDβ docks onto the NBD, and subsequently SBDα follows suit. Furthermore, bound substrates decrease the rate of SBDα-NBD docking, and this rate is surprisingly

much lower than peptide-dissociation rates, indicating that once SBDα contacts the NBD, substrates are no longer in the substrate binding pocket.

Several lines of evidence verify that our crystal structure represents an open conformation relevant for the ATP state of Hsp70s: (1) cysteines in only two positions in helix B (SBDα) formed efficiently intramolecular disulfide bonds to a cysteine in the NBD, indicating that these disulfide bonds are specific; (2) oxidized DnaK-E47C,F529C and DnaK-E47C,D526C exhibit tryptophane-fluorescence emission maxima similar to that of wild-type DnaK in the ATP-bound state; (3) cysteines in positions 167 and 480 in NBD and SBDβ, which are relatively close in our structure, are also able to form disulfide bonds; (4) fluorescence labels introduced in the different positions show an ATP-dependent quenching, indicating distances of less than 16 Å, consistent with our structure; and (5) many residues involved in interdomain contacts in our structure have been shown previously to be important for in vivo function of DnaK, and for some of these residues, it was demonstrated that replacement leads to a loss of allosteric control (see detailed discussion in the Supplemental Information).

This ATP-bound open conformation of Hsp70s resembles the conformation of their distant relatives and nucleotide exchange factors, Hsp110. Such a similarity was previously proposed (Liu and Hendrickson, 2007) and was supported by complementation assays. However, as discussed in detail in the Supplemental Information, there are significant differences between the structures. Our data indicate that Hsp70 is more dynamic in the ATP-bound state and that docking of the SBDα with the NBD is a transient event. Dissociation of this interaction is a prerequisite for the high substrate and DnaJ-stimulated ATPase rate. Sse1 seems to be frozen in this open conformation, and thereby to have lost its allosteric control mechanism.

Surprisingly, we discovered that Hsp70s can assume such an open conformation even in the ADP-bound and nucleotide-free states. These findings are consistent with the observation that substrate binding and release is possible in the absence of ATP (Schmid et al., 1994; Pierpaoli et al., 1998; Mayer et al., 2000b) and that the distance distribution in the high-affinity state includes a population with an SBDα-to-SBDβ distance of more than 25 Å (Marcinowski et al., 2011; Schlecht et al., 2011). However, it is completely unexpected that lid opening in the nucleotide-free state involves detachment of SBDα and docking of SBDα and SBDβ to different sites of the NBD. Note that detachment of SBDα from SBDβ is not necessary for substrate binding but for allosteric regulation, because a disulfide bridge between helix A of SBDα and SBDβ leads to a complete loss of allosteric regulation, but not loss of substrate binding (Schlecht et al., 2011). Our findings are consistent with a hypothesis proposed earlier that the difference between high-affinity and low-affinity states of Hsp70s is not the actual conformation but the frequency of transition between the open and closed conformations and their relative abundance (Mayer et al., 2000a). This is reflected in our fluorescence-quenching experiments, which indicated a closer average distance between SBDα and NBD and between SBDβ and NBD in the presence of ATP.

Based on these and previously published data from many laboratories, we propose the following action cycle for Hsp70 (Figure 7A). In the nucleotide-free state, closed and open conformation of Hsp70s are in equilibrium (see also Figure 3C), with a majority of molecules at any given time being closed. ATP-binding shifts this equilibrium toward the open conformation, whereby the subdomains of the NBD are rotated relative to the closed conformation to accommodate the interactions with the different regions of SBDβ. SBDα docks onto the NBD but, in contrast to the situation in Hsp110 chaperones, does not remain stably bound. Frequent excursions to the closed state occur. These are necessary for effective ATP hydrolysis, as evidenced by the reduced substrate and DnaJ-stimulated ATPase rates of oxidized DnaK-E47C,F529C (Figure 2B), and thus for substrate trapping. Substrate binding has two effects on the substrate binding site: (1) the substrate-enclosing loops come closer together due to hydrogen bonding with the backbone of the substrate, resulting in a narrowing of the angle between strands 1 and 4 of the SBDβ (see Movie S2); and (2) insertion of the central hydrophobic residue into the substrate binding pocket, which requires strands 3 and 4 to move apart (Figure 7B, Movie S3). Both changes are transmitted to the NBD-contacting residues, releasing the NBD-SBD linker as demonstrated earlier (Rist et al., 2006) and affecting the rotation of the NBD subdomains relative to each other. Concomitantly, the positions of γ-phosphate coordinating residues including Lys70 and Glu171 shift, which ultimately triggers γ-phosphate cleavage. ATP hydrolysis, in turn, allows further rotation of the NBD subdomains, thereby weakening the contact sites between NBD and SBDβ, and thus promotes dissociation of the two domains. Nucleotide exchange returns Hsp70 to the ground-state equilibrium.

How is ATP hydrolysis catalyzed by Hsp70s? In our structure, due to the subdomain rotation within the NBD, Lys70 is displaced by more than 2 Å as compared to all previous NBD structures of wild-type and mutant Hsp70s, and its amino group is positioned at H-bond distance to the γ-phosphate. This suggests that the function of Lys70 is to stabilize the pentavalent transition state of the phosphate during hydrolysis and not to position a water or hydroxyl ion for the inline attack as previously proposed (Flaherty et al., 1994; Wilbanks et al., 1994; O'Brien et al., 1996). Lys70 therefore has a similar function as the arginine finger in GTPases (Scheffzek et al., 1997) and other ATPases (Nadanaciva et al., 1999). In contrast, our structure suggests that Glu171, which is also displaced by almost 2 Å as compared to previous structures, coordinates the attacking water and acts as an acceptor for the released proton. Thr199, which is missing in our structure, may be involved in guiding the water to the γ-phosphate.

What is the function of DnaJ in this catalytic mechanism? Our ATPase assays with the oxidized DnaK-R167C,A480C suggest a hypothesis. Even in the absence of substrate and DnaJ, this variant had an ATPase rate that was almost as high as the substrate and DnaJ-stimulated ATPase rate of wild-type DnaK (Figure 2C). Substrate-induced release of the linker might weaken the SBDβ-NBD interaction, and binding of the J domain of DnaJ in the vicinity of Arg167, as suggested by genetic and biochemical data (Suh et al., 1998; Vogel et al., 2006), might clamp SBDβ and NBD together to prevent premature dissociation of the two domains. In oxidized DnaK-R167C,A480C,

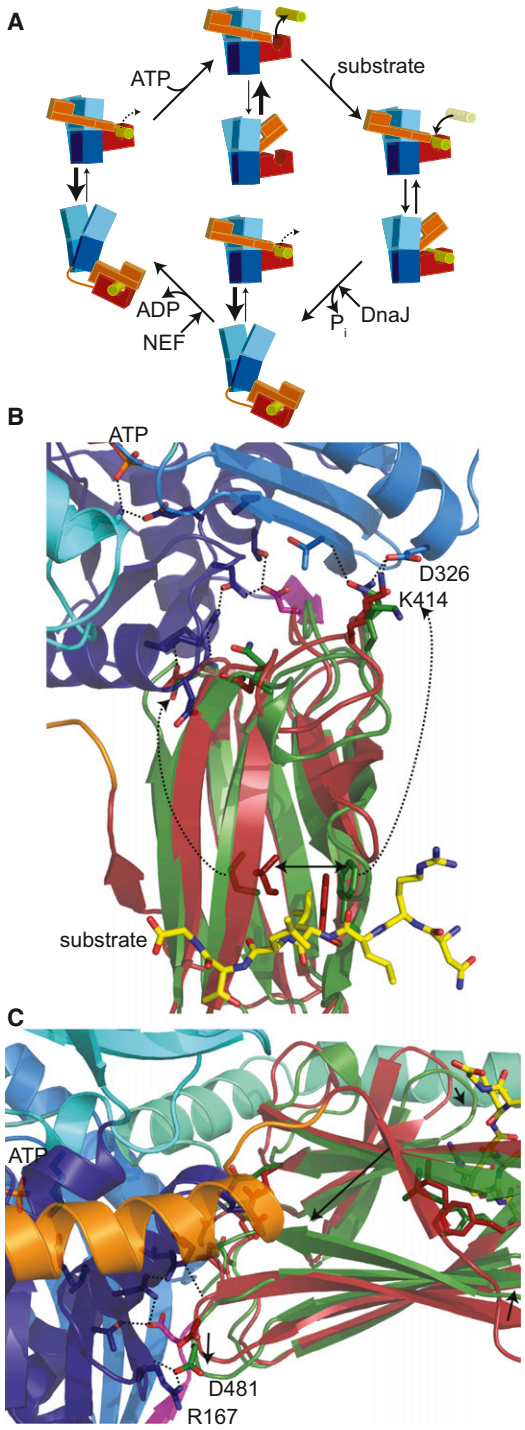

Figure 7. Model of Conformational Changes during the ATPase-Coupled Polypeptide Binding and Release Cycle of Hsp70s

(A) Cartoon of conformational equilibria of Hsp70s during the ATPase cycle. In all states, open and closed conformations are observed. Coloring of subdomains is as in Figure 1; NBD subdomains are shown in different shades of blue, SBDβ in brown, SBDα in orange, and substrate in yellow and light green. Thickness of the arrows signifies transition rates. Relocation of SBDα relative to SBDβ is coupled to subdomain rotations, shearing, and twisting motions in the NBD. NEF, nucleotide exchange factor.

(B and C), Proposed mechanism of substrate-stimulated ATP hydrolysis. Overlay of open substrate-free (brown, DnaK·ATP) and substrate-containing closed (green, PDB ID code 1DKX) conformations of SBDβ in the top (B) and side (C) views. Cocrystallized peptide is shown in yellow. SBDα in the open and closed conformation is shown in orange and light green, respectively. Dotted lines signify hydrogen-bonding distance; the dotted arrow indicates transmission direction from the substrate binding signal; solid arrows indicate movement upon substrate binding.

a dissociation of SBDβ and NBD is not possible, resulting in a high ATPase rate.

Our fluorescence data revealed additional insights into the mechanism of Hsp70s. Bound substrates slowed the SBDα-NBD docking rate significantly. Given that substrate dissociation rates were much higher than SBDα-NBD docking rates, substrates appear to affect the mechanics of the SBDβ to allow full interaction only after complete substrate dissociation. This finding may have very important implications for the regulation of the chaperone cycle of Hsp70s. The processed substrate must be able to escape before Hsp70 assumes a conformation competent for hydrolysis of the newly bound ATP. Otherwise, the substrate would be immediately entrapped by the chaperone for the next cycle, the substrate may not have a chance to reach the native state, and the chaperone may perform futile cycles of ATP hydrolysis. The fully opened lid may be an important signal for the NBD that the protein is in the optimal conformation for ATP hydrolysis. This assumption is consistent with the observation that ATPase activity of DnaK is poorly stimulated by substrate and DnaJ when the lid is cross-linked to the SBDβ (Schlecht et al., 2011). However, this hypothesis seems at odds with our ATPase experiments with oxidized DnaK-E47C,F529C, which is arrested in the SBDα-NBD-docked conformation and has lower ATPase rates in the presence of substrate and DnaJ than does wild-type DnaK or the same variant in the reduced state. Therefore, the docking of the SBDα may be a transient event necessary for allowing ATP to reach the hydrolysis competent position in the nucleotide binding pocket. Closing of the lid over the bound substrate may be the final signal that allows ATP hydrolysis. Such a mechanism would be most effective in trapping misfolded polypeptides.

EXPERIMENTAL PROCEDURES

Plasmids and Proteins

The *dnaK* mutants were constructed by site-directed mutagenesis (Kunkel et al., 1991) and expressed in pUHE21-2fdΔ12 (Buchberger et al., 1994) or in pMPM-A4 (Mayer, 1995). All DnaK variants were produced with a C-terminal His_6-tag in *E. coli* BB1553 strain (MC4100 *ΔdnaK52 sidB1*, Bukau and Walker, 1990) harboring plasmid pDMI.1(*lacI*^{q}) (Bujard and Lanzer, 1994) by induction with either 1 mM IPTG or 0.2% L-(+)-arabinose at 30°C. The protein was purified using Ni-IDA matrix (Protino, Macherey-Nagel), washed with Buffer A (40 mM Tris-HCl [pH 7.9], 100 mM KCl, 20 mM imidazol), and then washed with Buffer A containing 5 mM ATP and 5 mM $MgCl_2$. Bound proteins were eluted with 500 mM imidazol in Buffer A. Bound nucleotides were removed from the protein as described (Theyssen et al., 1996). His_6-σ^{32} was purified according to Arsène et al. (1999). DnaJ was a kind gift from Dr. F. Rodriguez.

Oxidation of Double-Cysteine Variants of DnaK

For formation of intramolecular disulfide bridges, the proteins were diluted in HKM buffer (25 mM HEPES-KOH [pH 7.6], 150 mM KCl, 5 mM $MgCl_2$) to a final

concentration of 2.5 μM and incubated with 0.5 mM Cu(II)-(1,10-Phenanthroline) complex at 30°C (Supplemental Experimental Procedures).

Crystallization of DnaK-E47C-T199A-F529C$_{ox}$ in the ATP-Bound State

DnaK-E47C,T199A,F529C was purified as described above with few modifications. After Ni-IDA purification, the protein was oxidized in the presence of 5 mM ATP, and the nucleotide was not removed. Subsequently, the protein was subjected to ion-exchange chromatography as described (Buchberger et al., 1994). For removal of the intermolecular crosslinking products from intramolecular ones, the protein was subjected to size-exclusion chromatography on the Superdex 200 (GE Healthcare) in HNKMG buffer (40 mM HEPES [pH 7.6], 100 mM NaCl, 20 mM KCl, 5 mM $MgCl_2$, 10% glycerol). Afterward, the protein was concentrated to 20 mg/ml and subjected to crystallization (for crystallization conditions, data collection, and refinement see Supplemental Experimental Procedures).

ATPase and Fluorescence Assays

ATPase Activity

Single-turnover ATPase rates were determined as described (Mayer et al., 1999).

Tryptophan Fluorescence

Tryptophan-emission spectra (300–400 nm) of DnaK (3 μM in HKM) were measured at an excitation wavelength of 295 nm on a PerkinElmer LS 55 spectrometer.

Probing the Relative Interdomain Distances

Fluorescence-emission spectra of HiLyte Fluor 488-labeled DnaK variants (1 μM in HKM buffer) were recorded from 500 to 580 nm (excitation 488 nm) at 30°C in the absence and in the presence of 1 mM ATP (Supplemental Experimental Procedures).

Kinetics of the ATP-Induced Conformational Changes

One micromolar of labeled DnaK alone or in complex with substrate was rapidly mixed 1:1 with 1 mM ATP in HKM buffer at 30°C in a stopped-flow device (SX.18 MV, Applied Photophysics; excitation wavelength 488 nm; cutoff filter 530 nm).

Peptide Dissociation Kinetics

Basal and ATP-induced peptide dissociation rates were determined as described previously, except that D-NR peptide (NRLLLTGC labeled with dansyl chloride) was used (Mayer et al., 2000b; Gässler et al., 2001).

ACCESSION NUMBERS

Coordinates and structure factors have been deposited in the RCSB Protein Data Bank with accession code 4B9Q.

SUPPLEMENTAL INFORMATION

Supplemental Information includes seven figures, two tables, three movies, Supplemental Discussion, and Supplemental Experimental Procedures and can be found with this article online at http://dx.doi.org/10.1016/j.molcel.2012.09.023.

ACKNOWLEDGMENTS

We would like to thank H. Lorenz, M. Boysen, R. Schlecht, N. Hentze, and L. Moullintraffort for advice on experiments and data analysis; F. Rodriguez for DnaJ protein; S. Hennes, S. Yücel, and E. Pirkl for technical assistance; C. Siegmann for support in the crystallization platform; and K. Wild for helpful discussions. This project was funded by the Deutsche Forschungsgemeinschaft (SFB638 and MA 1278/4-1 to M.P.M., and Cluster of Excellence: CellNetworks EXC 81/1). I.S. and M.P.M. are investigators of the Cluster of Excellence: CellNetworks.

Received: June 28, 2012
Revised: August 23, 2012
Accepted: September 27, 2012
Published online: November 1, 2012

REFERENCES

Arsène, F., Tomoyasu, T., Mogk, A., Schirra, C., Schulze-Specking, A., and Bukau, B. (1999). Role of region C in regulation of the heat shock gene-specific sigma factor of Escherichia coli, sigma32. J. Bacteriol. *181*, 3552–3561.

Barthel, T.K., Zhang, J., and Walker, G.C. (2001). ATPase-defective derivatives of Escherichia coli DnaK that behave differently with respect to ATP-induced conformational change and peptide release. J. Bacteriol. *183*, 5482–5490.

Bertelsen, E.B., Chang, L., Gestwicki, J.E., and Zuiderweg, E.R.P. (2009). Solution conformation of wild-type E. coli Hsp70 (DnaK) chaperone complexed with ADP and substrate. Proc. Natl. Acad. Sci. USA *106*, 8471–8476.

Buchberger, A., Valencia, A., McMacken, R., Sander, C., and Bukau, B. (1994). The chaperone function of DnaK requires the coupling of ATPase activity with substrate binding through residue E171. EMBO J. *13*, 1687–1695.

Bujard, H., and Lanzer, M. November 1994. Expression control sequences. U.S. patent 5362646.

Bukau, B., and Walker, G.C. (1990). Mutations altering heat shock specific subunit of RNA polymerase suppress major cellular defects of E. coli mutants lacking the DnaK chaperone. EMBO J. *9*, 4027–4036.

Dragovic, Z., Broadley, S.A., Shomura, Y., Bracher, A., and Hartl, F.U. (2006). Molecular chaperones of the Hsp110 family act as nucleotide exchange factors of Hsp70s. EMBO J. *25*, 2519–2528.

Flaherty, K.M., DeLuca-Flaherty, C., and McKay, D.B. (1990). Three-dimensional structure of the ATPase fragment of a 70K heat-shock cognate protein. Nature *346*, 623–628.

Flaherty, K.M., Wilbanks, S.M., DeLuca-Flaherty, C., and McKay, D.B. (1994). Structural basis of the 70-kilodalton heat shock cognate protein ATP hydrolytic activity. II. Structure of the active site with ADP or ATP bound to wild type and mutant ATPase fragment. J. Biol. Chem. *269*, 12899–12907.

Gässler, C.S., Wiederkehr, T., Brehmer, D., Bukau, B., and Mayer, M.P. (2001). Bag-1M accelerates nucleotide release for human Hsc70 and Hsp70 and can act concentration-dependent as positive and negative cofactor. J. Biol. Chem. *276*, 32538–32544.

Graf, C., Stankiewicz, M., Kramer, G., and Mayer, M.P. (2009). Spatially and kinetically resolved changes in the conformational dynamics of the Hsp90 chaperone machine. EMBO J. *28*, 602–613.

Hartl, F.U., Bracher, A., and Hayer-Hartl, M. (2011). Molecular chaperones in protein folding and proteostasis. Nature *475*, 324–332.

Kampinga, H.H., and Craig, E.A. (2010). The HSP70 chaperone machinery: J proteins as drivers of functional specificity. Nat. Rev. Mol. Cell Biol. *11*, 579–592.

Karzai, A.W., and McMacken, R. (1996). A bipartite signaling mechanism involved in DnaJ-mediated activation of the Escherichia coli DnaK protein. J. Biol. Chem. *271*, 11236–11246.

Kunkel, T.A., Bebenek, K., and McClary, J. (1991). Efficient site-directed mutagenesis using uracil-containing DNA. Methods Enzymol. *204*, 125–139.

Laufen, T., Mayer, M.P., Beisel, C., Klostermeier, D., Mogk, A., Reinstein, J., and Bukau, B. (1999). Mechanism of regulation of hsp70 chaperones by DnaJ cochaperones. Proc. Natl. Acad. Sci. USA *96*, 5452–5457.

Liu, Q., and Hendrickson, W.A. (2007). Insights into Hsp70 chaperone activity from a crystal structure of the yeast Hsp110 Sse1. Cell *131*, 106–120.

Marcinowski, M., Höller, M., Feige, M.J., Baerend, D., Lamb, D.C., and Buchner, J. (2011). Substrate discrimination of the chaperone BiP by autonomous and cochaperone-regulated conformational transitions. Nat. Struct. Mol. Biol. *18*, 150–158.

Mayer, M.P. (1995). A new set of useful cloning and expression vectors derived from pBlueScript. Gene *163*, 41–46.

Mayer, M.P., and Bukau, B. (2005). Hsp70 chaperones: cellular functions and molecular mechanism. Cell. Mol. Life Sci. *62*, 670–684.

Mayer, M.P., Laufen, T., Paal, K., McCarty, J.S., and Bukau, B. (1999). Investigation of the interaction between DnaK and DnaJ by surface plasmon resonance spectroscopy. J. Mol. Biol. *289*, 1131–1144.

Mayer, M.P., Rüdiger, S., and Bukau, B. (2000a). Molecular basis for interactions of the DnaK chaperone with substrates. Biol. Chem. *381*, 877–885.

Mayer, M.P., Schröder, H., Rüdiger, S., Paal, K., Laufen, T., and Bukau, B. (2000b). Multistep mechanism of substrate binding determines chaperone activity of Hsp70. Nat. Struct. Biol. *7*, 586–593.

McCarty, J.S., Buchberger, A., Reinstein, J., and Bukau, B. (1995). The role of ATP in the functional cycle of the DnaK chaperone system. J. Mol. Biol. *249*, 126–137.

Moro, F., Fernández, V., and Muga, A. (2003). Interdomain interaction through helices A and B of DnaK peptide binding domain. FEBS Lett. *533*, 119–123.

Nadanaciva, S., Weber, J., Wilke-Mounts, S., and Senior, A.E. (1999). Importance of F1-ATPase residue alpha-Arg-376 for catalytic transition state stabilization. Biochemistry *38*, 15493–15499.

O'Brien, M.C., Flaherty, K.M., and McKay, D.B. (1996). Lysine 71 of the chaperone protein Hsc70 Is essential for ATP hydrolysis. J. Biol. Chem. *271*, 15874–15878.

Pierpaoli, E.V., Gisler, S.M., and Christen, P. (1998). Sequence-specific rates of interaction of target peptides with the molecular chaperones DnaK and DnaJ. Biochemistry *37*, 16741–16748.

Raviol, H., Sadlish, H., Rodriguez, F., Mayer, M.P., and Bukau, B. (2006). Chaperone network in the yeast cytosol: Hsp110 is revealed as an Hsp70 nucleotide exchange factor. EMBO J. *25*, 2510–2518.

Rist, W., Graf, C., Bukau, B., and Mayer, M.P. (2006). Amide hydrogen exchange reveals conformational changes in hsp70 chaperones important for allosteric regulation. J. Biol. Chem. *281*, 16493–16501.

Scheffzek, K., Ahmadian, M.R., Kabsch, W., Wiesmüller, L., Lautwein, A., Schmitz, F., and Wittinghofer, A. (1997). The Ras-RasGAP complex: structural basis for GTPase activation and its loss in oncogenic Ras mutants. Science *277*, 333–338.

Schlecht, R., Erbse, A.H., Bukau, B., and Mayer, M.P. (2011). Mechanics of Hsp70 chaperones enables differential interaction with client proteins. Nat. Struct. Mol. Biol. *18*, 345–351.

Schmid, D., Baici, A., Gehring, H., and Christen, P. (1994). Kinetics of molecular chaperone action. Science *263*, 971–973.

Suh, W.C., Burkholder, W.F., Lu, C.Z., Zhao, X., Gottesman, M.E., and Gross, C.A. (1998). Interaction of the Hsp70 molecular chaperone, DnaK, with its cochaperone DnaJ. Proc. Natl. Acad. Sci. USA *95*, 15223–15228.

Swain, J.F., Dinler, G., Sivendran, R., Montgomery, D.L., Stotz, M., and Gierasch, L.M. (2007). Hsp70 chaperone ligands control domain association via an allosteric mechanism mediated by the interdomain linker. Mol. Cell *26*, 27–39.

Theyssen, H., Schuster, H.P., Packschies, L., Bukau, B., and Reinstein, J. (1996). The second step of ATP binding to DnaK induces peptide release. J. Mol. Biol. *263*, 657–670.

Vogel, M., Mayer, M.P., and Bukau, B. (2006). Allosteric regulation of Hsp70 chaperones involves a conserved interdomain linker. J. Biol. Chem. *281*, 38705–38711.

Wilbanks, S.M., and McKay, D.B. (1995). How potassium affects the activity of the molecular chaperone Hsc70. II. Potassium binds specifically in the ATPase active site. J. Biol. Chem. *270*, 2251–2257.

Wilbanks, S.M., DeLuca-Flaherty, C., and McKay, D.B. (1994). Structural basis of the 70-kilodalton heat shock cognate protein ATP hydrolytic activity. I. Kinetic analyses of active site mutants. J. Biol. Chem. *269*, 12893–12898.

Zhu, X., Zhao, X., Burkholder, W.F., Gragerov, A., Ogata, C.M., Gottesman, M.E., and Hendrickson, W.A. (1996). Structural analysis of substrate binding by the molecular chaperone DnaK. Science *272*, 1606–1614.